On the Discretization of Interface Problems with Perfect and Imperfect Contact

TATIANA CHERNOGOROVA   RICHARD EWING
OLEG ILIEV   RAYTCHO LAZAROV

Abstract

A second-order difference scheme for a first-order elliptic system with discontinuous coefficients is derived and studied. This approximation can be viewed as an improvement of the well-known scheme with harmonic averaging of the coefficients for a second order elliptic equation, which is first-order accurate for the gradient of the solution. The numerical experiments confirm the second order convergence for the scaled gradient, and demonstrate the advantages of the new discretization, compared with the older ones.

KEYWORDS: interface problems, second order discretization

1 Introduction

The single-phase fluid flow in a fully-saturated inhomogeneous porous media that occupies a bounded domain $\Omega \subset R^n,\ n = 1, 2, 3$ is often modeled by first-order system

$$\nabla \cdot \mathbf{u} = f(x), \quad \mathbf{u} = -K\nabla p \ \text{ for } \ x \in \Omega, \tag{1.1}$$

subject to various boundary conditions. Here $\mathbf{u}$ is the Darcy velocity, p is the pressure, and $K(x)$ is the permeability tensor. The first equation is the continuity equation, while the second one expresses the relation between the pressure gradient and the velocity by the linear Darcy law. We assume that $K(x)$ is a diagonal matrix with positive elements which may have jump

Lecture Notes in Physics
Chen, Ewing, and Shi (eds.), pp. 1–12.

put here ISBN

discontinuities across given surfaces Γ called interfaces. In this paper we consider two types of conditions on the interface Γ: (a) a perfect contact:

$$[p] = 0, \quad [\mathbf{u} \cdot \mathbf{n}] = 0 \quad \text{for} \quad \xi \in \Gamma; \tag{1.2}$$

and (b) imperfect contact:

$$(\mathbf{u} \cdot \mathbf{n})_+ = (\mathbf{u} \cdot \mathbf{n})_- = \alpha_\xi (p_+ - p_-) \quad \text{for} \quad \xi \in \Gamma. \tag{1.3}$$

Here $\mathbf{n}$ is the normal to the interface Γ unit vector (with fixed direction), $g_\pm(\xi)$ denotes the right and left limits of the function g at point ξ, and $[g] = g_+ - g_-$.

Often the velocity is eliminated so that the system (1.1) is reduced to a second-order elliptic equation for the pressure. A modified finite volume discretization for such a class of elliptic problems has been introduced and studied in [2, 3] and numerical experiments, confirming second-order convergence for the pressure, have been presented. In the present paper we continue the research in [2, 3] by introducing a new approximation of the velocity and studying its properties. We also study the relative accuracy for the approximate pressure near the interface, and discuss its superconvergent behavior in a particular case. We restrict our consideration to a class of interface problems for which: (1) each interface is parallel to a co-ordinate axes, and (2) the velocity is continuously differentiable in the normal direction to the interfaces. Under these two assumptions, we construct a second-order approximation of the system (1.1) on a staggered grid so that the pressure values are computed at the centers of the control volumes, while the values of the normal component of the velocity are computed at faces of the cells. The numerical experiments show that the derived scheme has second order convergence for both, the pressure and the velocity, and is superior to the schemes with harmonic averaging, which exhibit second-order convergence for the pressure and first order convergence for the velocity. The computations also show that for a smooth velocity the proposed discretization gives a considerably more accurate pressure, compared to the results of the scheme with harmonic averaging of the coefficients.

2 Discretization of the Interface Problem

Here we present in detail the discretization of the one-dimensional (1-D) problems with perfect and imperfect contacts. The discretization of the multidimensional problem on a tensor-product grid is just a tensor product of 1-D discretizations.

2.1 Discretization of the Perfect Contact Problem

In order to illustrate our approach, we first consider the perfect contact problem (1.1) - (1.2) in the one-dimensional case. We introduce a standard uniform cell–centered grid, $x_0 = 0, x_1 = h/2, x_i = x_{i-1} + h,\ i = 2, \cdots, N, x_{N+1} = 1$, where $h = 1/N$. The internal grid points can be considered as centered around the control volumes $V_i = (x_{i-\frac{1}{2}}, x_{i+\frac{1}{2}})$ where $x_{i+\frac{1}{2}} = x_i + \frac{1}{2}h,\ x_{i-\frac{1}{2}} = x_i - \frac{1}{2}h$. The values of the pressure and of the right hand side are defined at the grid points x_i and are denoted by p_i, f_i. The values of the velocity are defined at the points $x_{i+\frac{1}{2}}$ and are denoted by $u_{i+\frac{1}{2}}$. Non-uniform grids can be treated in a similar way. Note, our approach is defined locally, at a particular control volume level, and it can work with standard vertex-based grids as well.

The second-order discretization of the continuity equation in (1.1) is straightforward:

$$u_{i+\frac{1}{2}} - u_{i-\frac{1}{2}} = h\ \varphi_i, \quad \varphi_i = \frac{1}{h}\int_{x_{i-\frac{1}{2}}}^{x_{i+\frac{1}{2}}} f(x)dx,\ i = 1, 2, ..., N. \tag{2.1}$$

Next, consider the Darcy law, rewritten in the form

$$-\frac{\partial p}{\partial x} = \frac{u(x)}{k(x)},$$

and integrate this expression over the interval (x_i, x_{i+1}):

$$-(p_{i+1} - p_i) = -\int_{x_i}^{x_{i+1}} \frac{\partial p}{\partial x}dx = \int_{x_i}^{x_{i+1}} \frac{u(x)}{k(x)}dx. \tag{2.2}$$

We assume that the velocity $u(x)$ is two-times continuously differentiable on the interface, so it can be expanded around the point $x_{i+\frac{1}{2}}$ in Taylor series:

$$u(x) = u_{i+\frac{1}{2}} + (x - x_{i+\frac{1}{2}})\frac{\partial u_{i+\frac{1}{2}}}{\partial x} + \frac{(x - x_{i+\frac{1}{2}})^2}{2}\frac{\partial^2 u(\eta)}{\partial x^2},\ \ \eta \in (x_i, x_{i+1}). \tag{2.3}$$

After replacing the first derivative of the velocity at $x_{i+\frac{1}{2}}$ by a two-point backward difference, we get the following approximation of (2.2):

$$-(p_{i+1} - p_i) = u_{i+\frac{1}{2}} \int_{x_i}^{x_{i+1}} \frac{dx}{k(x)} + \frac{u_{i+\frac{1}{2}} - u_{i-\frac{1}{2}}}{h} \int_{x_i}^{x_{i+1}} \frac{(x - x_{i+\frac{1}{2}})}{k(x)}dx + O(h^3). \tag{2.4}$$

Finally, we rewrite this equation in the following basic form:

$$-k^H_{i+\frac{1}{2}} \frac{p_{i+1} - p_i}{h} = u_{i+\frac{1}{2}} + a_{i+\frac{1}{2}}(u_{i+\frac{1}{2}} - u_{i-\frac{1}{2}}) + \psi_i, \tag{2.5}$$

where $\psi_i = O(h^2)$ and

$$k^H_{i+\frac{1}{2}} = \left(\frac{1}{h} \int_{x_i}^{x_{i+1}} \frac{dx}{k(x)} \right)^{-1}, \quad a_{i+\frac{1}{2}} = k^H_{i+\frac{1}{2}} \frac{1}{h^2} \int_{x_i}^{x_{i+1}} \frac{x - x_{i+\frac{1}{2}}}{k(x)} dx. \tag{2.6}$$

Here $k^H_{i+\frac{1}{2}}$ is the well-known harmonic averaging of the coefficient $k(x)$ over the cell (x_i, x_{i+1}), which has played a fundamental role in deriving accurate schemes for discontinuous coefficients (see, e.g. [4, 5, 6, 7]). This presentation of the velocity $u(x)$ is a starting point for our discretization. Since we have assumed that the velocity is smooth, then the consecutive terms in the right-hand side in (2.5) are $O(1)$, $O(h)$ and $O(h^2)$, respectively. Truncation of this sum after the first term produces the well-known scheme of Samarskii [5] with harmonic averaging of the coefficient. This scheme is $O(h)$-consistent for the velocity at the interface points and second-order accurate for the pressure in the discrete H^1-norm. Further in the text, we call this scheme *harmonic averaging* or HA scheme.

Now we derive an $O(h^2)$ consistent scheme for the velocity by disregarding only the ψ_i-term in (2.5). We denote by P_i the approximate pressure at the grid points in order to distinguish it from the exact values p_i. Similarly, the approximate velocity is denoted by $U^-_{i+\frac{1}{2}}$, $U^+_{i-\frac{1}{2}}$ etc., where the sign $\pm$ indicates the right and left values of the flux at the point. Note, that the exact fluxes are continuous, while the approximate fluxes may have different $U^{\pm}_{i+\frac{1}{2}}$ values. Thus, we get

$$-k^H_{i+\frac{1}{2}} \frac{P_{i+1} - P_i}{h} = U^-_{i+\frac{1}{2}} + a_{i+\frac{1}{2}}(U^-_{i+\frac{1}{2}} - U^+_{i-\frac{1}{2}}), \tag{2.7}$$

$$-k^H_{i-\frac{1}{2}} \frac{P_i - P_{i-1}}{h} = U^+_{i-\frac{1}{2}} + a_{i-\frac{1}{2}}(U^-_{i+\frac{1}{2}} - U^+_{i-\frac{1}{2}}). \tag{2.8}$$

In summary, *the equations (2.1),(2.7), and (2.8) approximates the first-order system (1.1) with local truncation error $O(h^2)$.* Further, we refer to this approximation as a scheme with *improved harmonic averaging* or IHA scheme.

Now we transform the discretization to a more suitable form. Subtracting (2.8) from (2.7) we get

$$(1 + a_{i+\frac{1}{2}} - a_{i-\frac{1}{2}})(U^-_{i+\frac{1}{2}} - U^+_{i-\frac{1}{2}}) = -k^H_{i+\frac{1}{2}} \frac{P_{i+1} - P_i}{h} + k^H_{i-\frac{1}{2}} \frac{P_i - P_{i-1}}{h}. \tag{2.9}$$

Combining this with the discretization of the continuity equation (2.1), we obtain

$$-\left(1+a_{i+\frac{1}{2}}-a_{i-\frac{1}{2}}\right)^{-1}\frac{1}{h}\left(k^H_{i+\frac{1}{2}}\frac{P_{i+1}-P_i}{h}-k^H_{i-\frac{1}{2}}\frac{P_i-P_{i-1}}{h}\right)=\varphi_i. \quad (2.10)$$

On the other hand, solving the system (2.7), (2.8) for $U^-_{i+\frac{1}{2}}$ and $U^+_{i-\frac{1}{2}}$, we get

$$\begin{aligned} U^-_{i+\frac{1}{2}} &= \frac{-k^H_{i+\frac{1}{2}}\frac{P_{i+1}-P_i}{h}\left(1-a_{i-\frac{1}{2}}\right)-k^H_{i-\frac{1}{2}}\frac{P_i-P_{i-1}}{h}a_{i+\frac{1}{2}}}{1+a_{i+\frac{1}{2}}-a_{i-\frac{1}{2}}}, \\ U^+_{i-\frac{1}{2}} &= \frac{k^H_{i+\frac{1}{2}}\frac{P_{i+1}-P_i}{h}a_{i-\frac{1}{2}}-k^H_{i-\frac{1}{2}}\frac{P_i-P_{i-1}}{h}\left(1+a_{i+\frac{1}{2}}\right)}{1+a_{i+\frac{1}{2}}-a_{i-\frac{1}{2}}}. \end{aligned} \quad (2.11)$$

The new scheme approximates the velocity with second-order accuracy, *independently* of the positions of the discontinuity of the coefficient $k(x)$. The price we paid is the necessity to evaluate the expressions $k^H_{i+\frac{1}{2}}, k^H_{i-\frac{1}{2}}$ and $a_{i+\frac{1}{2}}, a_{i-\frac{1}{2}}$ with an error no larger than $O(h^2)$. Let a point ξ where the coefficient $k(x)$ is discontinuous be in the form $\xi = x_i + \theta h$ for some i and $0 \le \theta \le 1$. Now we consider particular realizations of this scheme. The approximation of the integral in $k^H_{i+\frac{1}{2}}$ is done by splitting it into integrals over (x_i, ξ) and (ξ, x_{i+1}) and then applying the trapezoidal rule for each integral. This approach will produce an accurate enough evaluation of $k^H_{i+\frac{1}{2}}$:

$$k^H_{i+\frac{1}{2}} \approx \left[\frac{\theta}{2}\left(\frac{1}{k_i}+\frac{1}{k_{\xi-0}}\right)+\frac{1-\theta}{2}\left(\frac{1}{k_{i+1}}+\frac{1}{k_{\xi+0}}\right)\right]^{-1}. \quad (2.12)$$

Note, that $k_{\xi-0}$ and $k_{\xi+0}$ are known from the interface condition.

Further, we continue with the second integral in (2.6). We again split the integral into two integrals and apply the trapezoidal rule for each of the two integrals:

$$\begin{aligned} \frac{1}{h^2}\int_{x_i}^{x_{i+1}}\frac{(x-x_{i+1})}{k(x)}dx &= \frac{1}{h^2}\int_{x_i}^{\xi}\frac{(x-x_{i+\frac{1}{2}})}{k(x)}dx \ + \ \frac{1}{h^2}\int_{\xi}^{x_{i+1}}\frac{(x-x_{i+\frac{1}{2}})}{k(x)}dx \\ &= \frac{\theta}{2}\left(\frac{\theta-0.5}{k_{\xi-0}}-\frac{0.5}{k_i}\right)+\frac{1-\theta}{2}\left(\frac{0.5}{k_{i+1}}+\frac{\theta-0.5}{k_{\xi+0}}\right) \ + \ O(h^2). \end{aligned} \quad (2.13)$$

In the case of a piece-wise constant coefficient $k(x)$ these formulas are exact and reduce to

$$k^H_{i+\frac{1}{2}} = \left(\frac{\theta}{k_i}+\frac{1-\theta}{k_{i+1}}\right)^{-1} \quad \text{and} \quad a_{i+\frac{1}{2}} = \frac{1}{2}\frac{\theta(1-\theta)(k_i-k_{i+1})}{(1-\theta)k_i+\theta k_{i+1}}. \quad (2.14)$$

Obviously, if the point of discontinuity ξ is a midpoint of the grid, i.e. $\xi = x_{i+\frac{1}{2}}$, then $\theta = 1/2$ so that (2.14) reduces to

$$k^H_{i+\frac{1}{2}} = 2\left(\frac{1}{k_i} + \frac{1}{k_{i+1}}\right)^{-1} \text{ and } a_{i+\frac{1}{2}} = \frac{1}{4}\left(\frac{k_i - k_{i+1}}{k_i + k_{i+1}}\right).$$

Remark 2.1 *Note that if $f(x) \equiv 1$ then $u''(x) = 0$ and the local truncation error is zero. Thus, HA scheme reproduces exactly piecewise linear solutions, while the IHA scheme reproduces exactly piecewise quadratic solutions.*

2.2 Discretization of the Imperfect Contact Problem

Discretization of imperfect contact problem in the case when interfaces are aligned with grid nodes, is studied in [6]. A harmonic averaging type of discretization for interfaces aligned with control volume faces has been discussed in [1]. Below we derive improved discretization for the case when interfaces are orthogonal to a co-ordinate axis. Consider the 1-D imperfect contact problem (1.1), (1.3). The discretization in this case is derived in a similar way as in the case of perfect contact, so we shall only list the final results. The second-order discretization of the continuity equation in (1.1) is almost the same as in the perfect contact case:

$$U^-_{i+\frac{1}{2}} - U^+_{i-\frac{1}{2}} = h\ \varphi_i, \quad \varphi_i = \frac{1}{h}\int_{x_{i-\frac{1}{2}}}^{x_{i+\frac{1}{2}}} f(x)dx, \ i = 1, 2, ..., N. \tag{2.15}$$

A second order consistent discretization to Darcy law is given by:

$$-\beta_{i+\frac{1}{2}}\frac{P_{i+1} - P_i}{h} = U^-_{i+\frac{1}{2}} + b_{i+\frac{1}{2}}(U^-_{i+\frac{1}{2}} - U^+_{i-\frac{1}{2}}). \tag{2.16}$$

For piecewise constant coefficients we have

$$b_{i+\frac{1}{2}} = (\theta - 0.5) + \frac{h\alpha_\xi}{2A_\xi}\left((1-\theta)^2 k_i - \theta^2 k_{i+1}\right),$$

where

$$A_\xi = k_i(1-\theta)h\alpha_\xi + k_{i+1}(k_i + \theta h\alpha_\xi), \quad k^H_{i+\frac{1}{2}} = \left[\frac{1-\theta}{k_{i+1}} + \frac{\theta}{k_i}\right]^{-1},$$

$$\beta_{i+\frac{1}{2}} = k^H_{i+\frac{1}{2}}\left(\frac{k^H_{i+\frac{1}{2}}}{h\alpha_{i+\frac{1}{2}}} + 1\right)^{-1}.$$

Note, in this particular case, we have second order of approximation for the velocity near the interface when $\theta \neq 0.5$, and third order of approximation for the velocity on the interface when $\theta = 0.5$.

3 Numerical Experiments

Numerical experiments were performed in order to study the behavior of the proposed discretization (IHA) and to compare it with the widely used discretization with harmonic averaging of the coefficients (HA). We approximately solve model problems with known analytical solution in order to assess the accuracy of the numerical solution. Three test problems have been considered. First, we solve a 2-D perfect contact problem with different permeabilities in 4 subregions, and investigate the cases when the interfaces are aligned with the control volume faces (i.e. $\theta = 0.5$), and when the grid is not aligned with the interfaces (i.e. $\theta \neq 0.5$). We show that IHA ensures second order convergence for the velocity in both cases, while HA is first-order accurate for the velocity in both cases. Both schemes are second-order accurate for the pressure, however the constant of convergence in IHA is much smaller. In the second test we solve a 2-D perfect contact problem with different permeabilities in 16 subregions. Superconvergence for the pressure (namely, accuracy of $O(h^3)$) is observed for this particular problem in the case of a constant permeability in the whole domain Ω. This is due to some symmetry and some cancellation of reminder terms. Numerical experiments show that for smooth velocity the IHA scheme preserves this superconvergence for the pressure in the case of discontinuous piecewise constant coefficients, while HA does not preserve it. Again, IHA ensures second-order accuracy for the velocity, while HA is only first-order accurate for the velocity. In the third example we solve a imperfect contact problem.

We should note that these computations do not guarantee high order of convergence for solutions with low regularity, for example, those produced by discontinuous coefficients and $f(x) \equiv 1$. Such solutions belong to the Sobolev space $H^{1+\gamma}(\Omega)$, where $\gamma > 0$ depends on the ratios of the jumps at the intersection points of the interfaces and can be very small.

Example 1. 2-D perfect contact problem in a unit square with interfaces at $x = \xi,\ y = \eta$ (4 subregions). The permeability is a piecewise constant in each sub-domain and takes values $k = \{10^{-2}, 1, 10^{-4}, 10^{+6}\}$ in the 4 subregions, counting from left to right and from bottom to top. The exact solution in this case is: $p^{ex} = \frac{1}{k} sin\left(\frac{\pi x}{2}\right)(x-\xi)(y-\eta)\left(1+x^2+y^2\right)$. Results from computations are presented in Table 1 and Table 2. The following notations are used: HA and IHA denote harmonic averaging based discretization and improved HA discretization for the case of aligned interfaces (i.e. $\theta = 0.5$), respectively. The notation "$\theta-$" in front of the scheme's notation is used when $\theta \neq 0.5$. Maximum errors for the pressure and their ratios are presented in Table 1. It is seen that both schemes converge with second order in both cases: aligned and non-aligned interfaces. The non-monotonic behavior of the convergence in the non-aligned case can be explained by the fact that θ varies from grid to grid, taking values larger or smaller than 0.5. In this way, the maximum value of the solution in different subregions is involved in the error estimate. Table 2 summarizes maximum errors for the velocity at the vertical interface (or at the nearest vertical line $x = x_{i+\frac{1}{2}}$ in the non-aligned case). It is clearly seen that IHA is second-order accurate for the velocity, while HA is only first-order accurate for it. Again non-monotone behavior of the convergence, related to alternating values for θ on the consecutive grids, is observed. A monotone convergence will be observed for fixed θ, for example, on grids contains $12 \times 12, 42 \times 42, 162 \times 162$ nodes.

Table 1. Maximum errors for pressure and their ratios

Example 1. 2-D perfect contact problem with 4 subregions;

	$\xi = \frac{1}{2}, \eta = \frac{1}{2}$, (aligned)				$\xi = \frac{1}{3}, \eta = \frac{1}{3}$, (non-aligned)			
Grid	HA scheme		IHA scheme		θ-HA scheme		θ-IHA scheme	
12x12	1.75d-2	-	3.34d-4	-	1.91d-2	-	4.48d-4	-
22x22	5.97d-3	*2.9*	7.64d-5	*4.4*	9.56d-3	*2.0*	1.45d-4	*3.1*
42x42	1.80d-3	*3.3*	1.94d-5	*3.9*	2.10d-3	*4.6*	4.02d-5	*3.6*
82x82	5.03d-4	*3.6*	4.97d-6	*3.9*	7.03d-4	*3.0*	1.10d-5	*3.7*
162x162	1.36d-4	*3.7*	1.26d-6	*3.9*	1.64d-4	*4.3*	2.80d-6	*3.9*
322x322	3.56d-5	*3.8*	3.17d-7	*4.0*	4.69d-5	*3.5*	7.19d-7	*3.9*

Table 2. Maximum errors for velocity and their ratios

Example 1. 2-D perfect contact problem with 4 subregions;

	$\xi = \frac{1}{2}, \eta = \frac{1}{2}$, (aligned)				$\xi = \frac{1}{3}, \eta = \frac{1}{3}$, (non-aligned)			
Grid	HA scheme		IHA scheme		θ-HA scheme		θ-IHA scheme	
12x12	4.20d-2	-	1.18d-3	-	2.19d-2	-	5.26d-4	-
22x22	2.14d-2	*1.96*	2.73d-4	*4.3*	2.83d-2	*0.77*	1.27d-4	*4.1*
42x42	1.08d-2	*1.98*	8.07d-5	*3.4*	5.62d-3	*5.03*	5.30d-5	*2.4*
82x82	5.40d-3	*2.00*	2.20d-5	*3.7*	7.11d-3	*0.79*	5.44d-6	*9.7*
162x162	2.70d-3	*2.00*	5.77d-6	*3.8*	1.41d-3	*5.04*	3.93d-6	*1.4*
322x322	1.35d-3	*2.00*	1.50d-6	*3.8*	1.78d-3	*0.79*	3.77d-7	*10.*

Example 2. 2-D perfect contact problem in a unit square with interfaces at $x = \xi_1 = 0.2, \quad x = \xi_2 = 0.5, \quad x = \xi_3 = 0.7$ and $y = \eta_1 = 0.3, \quad y = \eta_2 = 0.6, \quad y = \eta_3 = 0.8$ (16 subregions). The permeability is

a piecewise constant function and in each sub-domain and takes values $k = 10 \times \{10, 10^{-3}, 1, 10^{-4}, 10^{-2}, 10, 10^{-3}, 1, 10, 10^{-3}, 1, 10^{-3}, 10^{-3}, 10, 10^{-2}, 1\}$ in the 16 subregions, counting from left to right and from bottom to top with exact solution $p(x,y) = \frac{1}{k}\,(x-\xi_1)\,(x-\xi_2)\,(x-\xi_3)\,(y-\eta_1)\,(y-\eta_2)\,(y-\eta_3)$. The computational results are presented in Tables 3 and 4. For comparison we have included also the results for the constant coefficient $k(x,y) = 1$ in the whole domain Ω. Notation "case B" is used to denote columns with these results. One can observe superconvergence for the pressure in the continuous case, which is also exhibited by IHA in the case of discontinuous coefficients. Table 4 shows that IHA ensures second-order convergence for the velocity, while HA is only first-order accurate. In our numerical experiments the exact solution is zero at the interfaces, so the absolute values for the error there might be small, compared to absolute errors far from interfaces, while the relative errors can be very large. So in Figures 1 and 2, we plot the relative error $\frac{p(x_i,y_j)-P_{i,j}}{p(x_i,y_j)}$ computed by HA and IHA, respectively. Here (x_i, y_j) are the centers of the cells in the rectangular grid. Qualitatively, the results look similar, but quantitatively they differ by orders of magnitude. The results show that IHA produces a considerably more accurate solution near the interface.

Example 3. 1-D imperfect contact problem with interfaces at $\xi_1 = 0.2$ and $\xi_2 = 0.7$ with an exact solution:

$$p(x) = -\frac{d}{k(s+1)(s+2)}x^{s+2} - \frac{c}{2k}x^2 + ax + b.$$

The parameters k, c, d vary for the different subregions. The constants in the imperfect contact interface conditions are $\alpha_1 = 10^2$, $\alpha_2 = 10$. Also, $u(0) = 1$, $u(1) = 0$, and $s = \{1, 1, 1\}$, $k = \left\{1, 10, 10^2\right\}$, $c = \left\{10, 1, 10^2\right\}$, in the three subregions, counting from the left.

Table 3. Maximum errors for pressure and their ratios

Example 2. 2-D perfect contact problem with 16 subregions;

Grid	$k(x,y) \equiv 1$ case B		aligned HA scheme		aligned IHA scheme	
12x12	1.75d-3	-	3.91d-3	-	1.65d-3	-
22x22	2.89d-4	*6.06*	1.49d-3	*2.62*	2.87d-4	*5.75*
42x42	4.18d-5	*6.91*	5.07d-4	*2.93*	4.17d-5	*6.88*
82x82	5.64d-6	*7.41*	1.55d-4	*3.27*	5.63d-6	*7.41*
162x162	7.33d-7	*7.69*	4.39d-5	*3.53*	7.32d-7	*7.69*
322x322	9.34d-8	*7.85*	1.19d-5	*3.69*	9.35d-8	*7.83*

Table 4. Maximum errors for velocity and their ratios

EXAMPLE 2. 2-D perfect contact problem with 16 subregions;

Grid	$k(x,y) \equiv 1$ case B		aligned HA scheme		aligned IHA scheme	
12x12	1.74d-4	-	2.02d-3	-	9.37d-4	-
22x22	5.85d-5	*2.97*	1.17d-3	*1.73*	2.91d-4	*3.21*
42x42	1.67d-5	*3.50*	6.20d-4	*1.89*	8.22d-5	*3.54*
82x82	4.42d-6	*3.77*	3.18d-4	*1.95*	2.39d-5	*3.44*
162x162	1.14d-6	*3.88*	1.60d-4	*1.99*	6.56d-6	*3.62*
322x322	2.89d-7	*3.94*	8.06d-5	*1.99*	1.75d-6	*3.75*

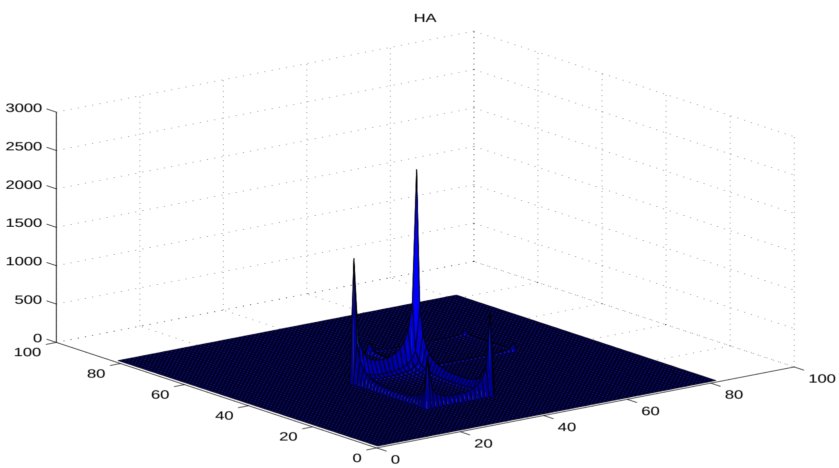

Fig. 1. THE RELATIVE ERROR IN EXAMPLE 2: HA SCHEME

Table 5. Maximum errors and their ratios

EXAMPLE 3. 1-D imperfect contact problem with 3 subregions.

Grid	PRESSURE HA scheme		PRESSURE IHA scheme		VELOCITY HA scheme		VELOCITY IHA scheme	
12x12	4.56d-3	-	2.47d-3	-	3.87d-2	-	2.49d-2	-
22x22	1.33d-3	*3.4*	5.12d-4	*4.8*	9.70d-3	*4.0*	5.46d-3	*4.6*
42x42	3.58d-4	*3.7*	9.77d-5	*5.2*	2.43d-3	*4.0*	1.11d-3	*4.9*
82x82	9.24d-5	*3.9*	1.83d-5	*5.3*	6.07d-4	*4.0*	2.50d-4	*5.4*
162x162	2.35d-5	*3.9*	3.27d-6	*5.6*	1.52d-4	*4.0*	3.55d-5	*5.8*
322x322	5.92d-6	*4.0*	5.84d-7	*5.6*	3.80d-5	*4.0*	6.04d-6	*5.9*

The results from computations are presented in Table 5. As it was mentioned in Section 2.2 the IHA scheme approximates velocity at the interface with third-order accuracy in the case when the imperfect contact interface is

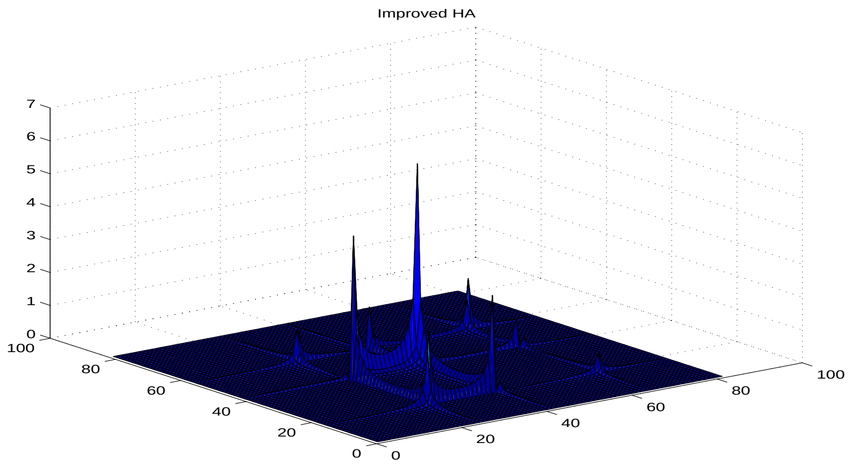

Fig. 2. The relative error in Example 2: IHA scheme

aligned with cell faces. In this case, the HA scheme approximates the velocity at the interface to second order. This may explain the second-order convergence for the HA scheme, and the superconvergence for the IHA scheme.

Acknowledgments. The work of the first and the third authors has been supported partially by Bulgarian FSI under grant MM-811. Part of the work of the second and the fourth author has been supported by the USA EPA Grant R 825207-01-1.

References

[1] Angot, Ph., Modeling and visualization of thermal fields inside electronic systems under operating conditions, *IBM Technical Report*, **TR-47095**, 70 (1989).

[2] Chernogorova, T. and Iliev, O., A 2nd order discretization of imperfect contact problems with piecewise constant coefficients on cell-centered grids, to appear in: *Notes in Numerical Fluid Mechanics*, M. Griebel et al (Eds), Proc. of Workshop on Large Scale Scientific Computations, June 1999, Sozopol, Bulgaria.

[3] Ewing, R., Iliev, O., and Lazarov, R., A modified finite volume approximation of second order elliptic equations with discontinuous coefficients, TR ISC-99-01-MATH, Texas A&M University, 1999 (submitted).

[4] Marchuk, G.I., *Methods of computational mathematics*, Moscow, Nauka, 1980.

[5] Samarskii, A.A., *Theory of difference schemes*, Moscow, Nauka, 1977.

[6] Samarskii, A.A. and Andréev, V.B., *Finite difference methods for elliptic problems*, Nauka Moscow, 1976 (in Russian), *Méthodes aux Différences pour Équations Elliptiques*, and MIR Moscou, 1978 (in French).

[7] Wesseling, P., *An Introduction to Multigrid Methods*, Wiley, N.Y., 1991.

Tatiana Chernogorova
Faculty of Mathematics and Informatics
The Sofia University St. Kl. Ohridski
5 J.Bouchier bul.
BG-1163 Sofia, Bulgaria
chernogorova@fmi.uni-sofia.bg

Richard Ewing
Institute for Scientific Computation
Texas A&M University,
College Station, TX 77843, USA
ewing@isc.tamu.edu

Oleg Iliev
Institute for Industrial Mathematics (ITWM)
Erwin-Schroedinger str., bld. 49
D-67663 Kaiserslautern, Germany
iliev@itwm.uni-kl.de

Raytcho Lazarov
Department of Mathematics
Texas A&M University,
College Station, TX 77843-3368, USA
lazarov@math.tamu.edu